



**HAL**  
open science

## Method for Controlling the PWM Switching: Application to Magnetic Noise Reduction

Jean-Francois Brudny, Tifany Szkudlapski, Fabrice Morganti, Jean-Philippe  
Lecointe

► **To cite this version:**

Jean-Francois Brudny, Tifany Szkudlapski, Fabrice Morganti, Jean-Philippe Lecointe. Method for Controlling the PWM Switching: Application to Magnetic Noise Reduction. IEEE Transactions on Industrial Electronics, 2015, 62 (1), pp.122-131. 10.1109/TIE.2014.2327583 . hal-04293982

**HAL Id: hal-04293982**

**<https://hal.science/hal-04293982>**

Submitted on 15 Jan 2024

**HAL** is a multi-disciplinary open access archive for the deposit and dissemination of scientific research documents, whether they are published or not. The documents may come from teaching and research institutions in France or abroad, or from public or private research centers.

L'archive ouverte pluridisciplinaire **HAL**, est destinée au dépôt et à la diffusion de documents scientifiques de niveau recherche, publiés ou non, émanant des établissements d'enseignement et de recherche français ou étrangers, des laboratoires publics ou privés.

# Method for Controlling the PWM Switching: Application to Magnetic Noise Reduction

Jean-François Brudny, *Senior Member, IEEE*, Tifany Szkudlapski, Fabrice Morganti, and Jean-Philippe Lecoite, *Member, IEEE*

**Abstract**—This paper presents an analytical method that makes it possible to define the pulsewidth modulation (PWM) supply output voltage spectral content, particularly the harmonic phase sequences, without switching instant determination. The results obtained from these developments lead to define a PWM control strategy that allows deleting some switching harmonics in order to reduce undesirable effects. Numerical studies and experiments confirm the theoretical approach and this harmonic control strategy.

**Index Terms**—Alternating current (ac) variable-speed drives, noise of magnetic origin, pulsewidth modulation (PWM) supply, switching harmonic control.

## I. INTRODUCTION

THE inverters supplying alternating-current electrical rotating machines are commonly used for many industrial applications [1]. If the sinus–triangle pulsewidth modulation (PWM) is still widely used [2], new techniques, such as space vector PWM (SVPWM), have been developed [3]. However, the use of such converters generates some undesirable effects tied to the switching three-phase harmonic (STPH) systems. Some of them concern additional losses [4], the acoustic noise of magnetic origin [5], [6], and the overvoltages induced in the windings, leading to the premature aging of the electrical insulation system [7]. To get away from these effects, the simplest solution consists of adding a filter at the inverter outputs. However, because of their cost and their dimensions, they are not always compatible with the industrial constraints. That is why the inverter output signals can be directly modified with multilevel converters, for example [8].

The magnetic noise is mainly generated by Maxwell’s forces, which result from the square of the air-gap flux density wave, composed of the fundamental and harmonic components due to the toothing and the switching. The double products, which combine the fundamental with the harmonics, are at the origin of phenomenon vibration, leading to acoustic effects that are particularly annoying if the force frequencies are close to the natural resonances of the stator. There are many studies [3] about the reduction of this noise, with appropriate PWM

strategies [9], [10]. Some of them increase the switching frequency [11] or use random PWM techniques [12]–[14]. Leleu *et al.* [15] compared the generalized discontinuous PWM, the homopolar 3 PWM, and the SVPWM in order to obtain the more silent machine. A technique called harmonic injection PWM–frequency-modulated triangular carrier to act on the reference and the carrier is given in [16]. It is also possible to adapt the machine to the switching effects [17] or to modify the mechanical structure response [18]. In [19], piezoelectric actuators are controlled to generate effects opposed the stator external vibrations. A new magnetic circuit structure presented in [20] allows reducing all the magnetic noise components.

This paper concerns the control of the switching effects on the magnetic noise and, more particularly, the definition of a PWM control strategy for suppressing a force component. That is obtained by suppressing the STPH that generates the force. To do that, the authors show that, for the classical sinus–triangle PWM, the spectral content of the voltages delivered by the inverter can be controlled by choosing appropriate three-phase triangular carriers that make the homopolar an intermediate STPH system, leading to delete the output annoying STPH. The problem requires characterizing the switching harmonic components not in terms of magnitude but in terms of phase sequences.

The first part presents an analytical method for modeling the PWM output voltages without switching instant determination. It is built by considering sinusoidal carriers (sinus–sinus PWM) in order to determine the harmonic phase sequences. The results, which are validated with numerical simulations and experiments, are extended to the sinus–triangle PWM to demonstrate that the analytical relationships are also valuable in this case. Upper indices “s” for a sinusoidal carrier and “ $\Delta$ ” for a triangular carrier will be used to distinguish the variables according to the carrier waveforms. No index means that the relations are valuable whatever the case. The second part is dedicated to the switching voltage harmonic control. The authors show how any rotating STPH system can be canceled by using three different appropriate carriers. Experiments considering the sinus–triangle PWM validate the theoretical approach and the STPH control strategy. The last part presents results that show the impact of this strategy on the radial vibrations of an induction machine.

## II. PWM MODELING

Let us denote  $v_q^{\text{ref}}$  and  $v_{cq}^{\Delta}$  as phase  $q$ ’s ( $q = 1, 2, \text{ or } 3$ ) sinusoidal reference and triangular carrier signals, respectively, whose angular frequencies are  $\omega$  (frequency  $f$ ) and  $m\omega$  (frequency

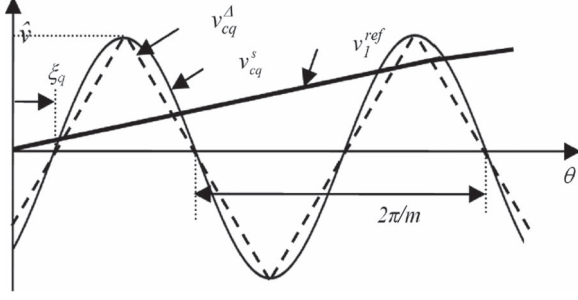


Fig. 1. PWM with triangular and sinusoidal carriers.

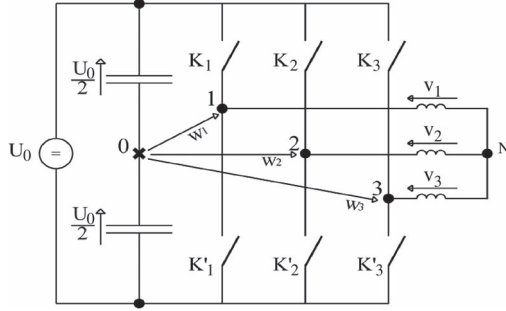


Fig. 2. Three-phase PWM inverter.

$f_{\text{PWM}} = mf$ ), respectively, where  $m$  is defined as the modulation index. In order to easily determine the PWM three-phase  $v_q$  output voltage characteristics, a  $v_{cq}^s$  sinusoidal carrier is substituted to  $v_{cq}^\Delta$ ; these two signals present the same peak values, as shown in Fig. 1. The analytical study is done considering that the  $r$  adjusting coefficient is equal to the unit. In the following, the time referential is linked to  $v_1^{\text{ref}}$  as it appears in Fig. 1. Thus,  $v_q^{\text{ref}}$  and  $v_{cq}^s$  can be expressed as:

$$v_q^{\text{ref}} = \hat{v} \sin(\theta - \phi_q) \quad (1)$$

$$v_{cq}^s = \hat{v} \sin[m(\theta - \xi_q)] \quad (2)$$

where  $\theta = \omega t$ , and  $\phi_q = (q-1)2\pi/3$ .  $\xi_q$  is phase  $q$ 's adjustable carrier phase difference. For the classical PWM,  $\xi_q$  is the same for whatever  $q$  is. Fig. 2 presents the three-phase inverter and the main notations.

- The control strategy is similar to that defined for the classical sinus-triangle PWM when  $v_q^{\text{ref}} > v_{cq}^s$ , the  $K_q$  switch is closed, and  $w_q^s = U_0/2$ ; for  $v_q^{\text{ref}} < v_{cq}^s$ ,  $K'_q$  is closed, and  $w_q^s = -U_0/2$ . The inequality  $v_q^{\text{ref}} > v_{cq}^s$ , taking into account (1) and (2), can be written as

$$\cos\left[\frac{(m+1)\theta - \phi_q - m\xi_q}{2}\right] \sin\left[\frac{(m-1)\theta + \phi_q - m\xi_q}{2}\right] \leq 0. \quad (3)$$

Let us introduce the  $f_a$  and  $f_b$  logic functions defined as follows.

- $f_a = 1$  or 0 if the cosine is positive or negative, respectively.
- $f_b = 1$  or 0 if the sine is negative or positive, respectively.

It can be shown that the  $w_q^s$  three-phase intermediate system can be expressed as

$$w_q^s = U_0(2f_a f_b - f_a - f_b + 1/2). \quad (4)$$

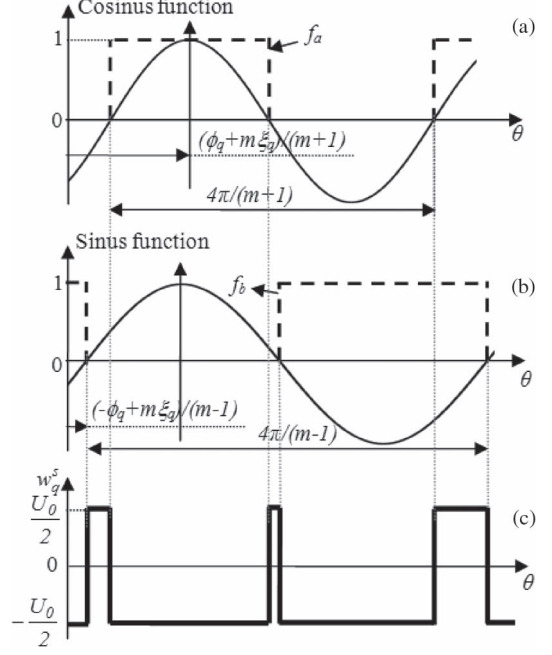


Fig. 3. Principle of the  $w_q^s$  determination.

Fig. 3 shows the principle applied to determine  $w_q^s$ . The  $f_a$  and  $f_b$  Fourier series can be written as

$$\left. \begin{aligned} f_a &= \frac{1}{2} + \frac{2}{\pi} \sum_{n_1=0}^{\infty} \frac{(-1)^{n_1}}{2n_1+1} \cos\left\{\frac{2n_1+1}{2}[(m+1)\theta - \phi_q - m\xi_q]\right\} \\ f_b &= \frac{1}{2} + \frac{2}{\pi} \sum_{n_2=0}^{\infty} \frac{-1}{2n_2+1} \sin\left\{\frac{2n_2+1}{2}[(m-1)\theta + \phi_q - m\xi_q]\right\} \end{aligned} \right\} \quad (5)$$

where  $n_1$  and  $n_2$  are positive or null integers. Let us denote  $W_0^s = -4U_0/\pi^2$ . Considering (5),  $w_q^s$  can be expressed as

$$w_q^s = \sum_{n_1=0}^{\infty} \sum_{n_2=0}^{\infty} (w_{q(k_1)}^s - w_{q(k_2)}^s) \quad (6)$$

where

$$\left. \begin{aligned} w_{q(k_1)}^s &= \hat{w}_{(k_1)}^s \sin(k_1\theta - N^-\phi_q - mN^+\xi_q) \\ w_{q(k_2)}^s &= \hat{w}_{(k_2)}^s \sin(k_2\theta - N^+\phi_q - mN^-\xi_q) \end{aligned} \right\} \quad (7)$$

$$\left. \begin{aligned} N^+ &= 1 + n_1 + n_2 \\ N^- &= n_1 - n_2 \end{aligned} \right\} \quad (8)$$

$$\left. \begin{aligned} k_1 &= mN^+ + N^- \\ k_2 &= mN^- + N^+ \end{aligned} \right\} \quad (9)$$

$$\hat{w}_{(k_1 \text{ or } k_2)}^s = (-1)^{n_1} W_0^s / [(2n_1+1)(2n_2+1)]. \quad (10)$$

Elementary considerations on  $\hat{w}_{(k_1 \text{ or } k_2)}^s$  make it possible to show that a harmonic of  $k$ -rank belongs to the  $k_1$  or  $k_2$  group only considering one term corresponding to the  $[n_1, n_2]$  couple, which carries the highest weight (smallest  $n_1$  and  $n_2$  values compared with the rest of the other concerned couples). Thus, (6) can be written as

$$w_q^s = \sum_k w_{q(k)}^s = \sum_{k_1} w_{q(k_1)}^s - \sum_{k_2} w_{q(k_2)}^s. \quad (11)$$

- These STPH systems are defined by their phase sequences: clockwise (C), anticlockwise (A), and homopolar (H). As for a balanced and star-connected load, i.e.,  $v_q = (2w_q - w_{q+1} - w_{q+2})/3$ , it is possible to consider a similar relationship for each  $k$  harmonic. As for the (C) and (A) systems,  $\sum_q w_{q(k)} = 0$ , and it can be deduced that

$$\left. \begin{aligned} v_{q(k)} &= w_{q(k)}, & \text{for (C) and (A) systems} \\ v_{q(k)} &= 0, & \text{for (H) systems} \end{aligned} \right\}. \quad (12)$$

One can first note that these developments are valid whatever the PWM is, i.e., synchronous or asynchronous. Then, it shows that a homopolar intermediate STPH system disappears from the output signals. It is also true, in the steady state, for a load that is delta connected by considering the equivalent star-connected load.

- It appears that this analytical model has considerable advantages because it makes it possible to determine the  $w_q^s$  (or  $v_q^s$ ) spectral contents and the harmonic phase sequences without calculating the switching instants. As some  $k_2$  values lead to STPH systems of negative frequency, their phase sequence determination is done by first considering  $k_2$  positive; then, for negative  $k_2$ , (C) is replaced by (A), and vice versa.

The problem now is to analyze under what conditions these results are applicable for the sinus-triangle PWM and how the  $r$  value affects this property established for  $r = 1$ . The developments will be done considering a synchronous PWM.

### III. VALIDATION OF PWM MODELING

The validation concerns the  $v_q$  spectral content for sinusoidal  $v_q^{\text{ref}}$ , where  $m = 55$ ,  $f = 50$  Hz, and  $U_0 = 520$  V, and a single carrier wave by comparing analytical, numerical, and experimental results for  $r = 1$  and then for  $r \neq 1$ .

All the experiments are made by connecting to the inverter outputs a three-phase star-connected 50-Hz 15-kW two-pole-pair cage induction machine operating at no load. The switching is controlled with a Focusrite sound card programmed with the Csound language. It allows generating single (or multiple) carrier(s) with a sinusoidal (or triangular) shape. A spectrum analyzer allows providing the  $v_q$  spectral content, both in amplitude and phase. Numerical results are obtained using a fast Fourier transform (FFT) made with Matlab or a computer program, which determines the different quantities from the switching instants.

#### A. Single Sinusoidal Carrier

- For  $r = 1$ , the  $w_q^s$  analytical harmonic ranks and phase sequences are given in Table I for the first  $n_1$  and  $n_2$  values. The  $\delta|\hat{w}_{q(k)}^s|$  corresponding absolute relative amplitudes deduced from (10), which are defined as percentage, are given by

$$\delta|\hat{w}_{q(k)}^s| = 100 \left| \frac{\hat{w}_{q(k)}^s}{\hat{w}_{q(1)}^s} \right| = 100 / [(2n_1 + 1)(2n_2 + 1)]. \quad (13)$$

TABLE I  
ANALYTICAL RANKS AND PHASE SEQUENCES OF  $w_q^s$  HARMONICS

		$k_1$ group							
$n_1$		0		1		2		3	
	0	$m$	(H)	$2m+1$	(C)	$3m+2$	(A)	$4m+3$	(H)
	1	$2m-1$	(A)	$3m$	(H)	$4m+1$	(C)	$5m+2$	(A)
$n_2$	2	$3m-2$	(C)	$4m-1$	(A)	$5m$	(H)	$6m+1$	(C)
	3	$4m-3$	(H)	$5m-2$	(C)	$6m-1$	(A)	$7m$	(H)
		$k_2$ group							
$n_1$		0		1		2		3	
	0	1	(C)	$m+2$	(A)	$2m+3$	(H)	$3m+4$	(C)
	1	$-m+2$	(C)	3	(H)	$m+4$	(C)	$2m+5$	(A)
$n_2$	2	$-2m+3$	(H)	$-m+4$	(A)	5	(A)	$m+6$	(H)
	3	$-3m+4$	(A)	$-2m+5$	(C)	$-m+6$	(H)	7	(C)

Thus,  $\delta|\hat{w}_{q(k)}^s|$  very quickly decreases when  $n_1$  and  $n_2$  increase so that the analysis may only cover the first  $n_1$  and  $n_2$  values.

- The  $v_q^s$  characteristics experimentally obtained for  $\xi_q = 0$  are given in Fig. 4, where the bold lines correspond to the terms resulting from the  $k_1$  group (deduced from the analytical study). The relative amplitudes, which are defined by a similar expression as (13), are given in Fig. 4(a), where  $\hat{v}_{q(1)}^s = |W_0^s| = 210.75$  V. A cross spectrum of  $v_{1(k)}^s$  and  $v_{2(k)}^s$  is made with a Bruël & Kjaer PULSE analyzer platform. It gives the phase differences presented in Fig. 4(b) for the main components ( $\delta|\hat{v}_{q(k)}^s| > 3\%$ ). Let us point out that a 0 difference corresponds to an (H) system; a  $2\pi/3$  difference, to a (C) system; and a  $4\pi/3$  difference, to an (A) system. There is no (H) system according to (12).

It appears that the number of components from the  $k_1$  group is very limited and that these components only appear in the harmonics families centered on  $m$  multiples.

Analytical and experimental results are in excellent correlation. It validates the theoretical results and the hypothesis that consists of using the relation (11) instead of the relation (6) to express  $w_q^s$ .

- The characteristics of the main harmonics have been calculated for different values of  $\xi_q$  and  $r$ .
  - For  $r = 1$ , the previous relative amplitudes are found, whatever the values of  $\xi_q$  are. For the phases, the analytical and numerical values, for a given value of  $\xi_q$ , are almost the same, with the error being increased with  $m$ . For example, the error obtained with the FFT is inferior to  $1^\circ$  for the  $3m+4$  component, and it is lower when the switching instants are calculated. Due to the numerical errors, it can be underlined that considering the term of a higher weight is perfectly justified to analytically characterize a harmonic.
  - $r \neq 1$  leads to a similar spectral content obtained than for  $r = 1$ , with differences on the relative amplitudes (the reference value is the fundamental component magnitude obtained for the considered  $r$  value). However, a notable result appears concerning the phases and, therefore, the phase sequences that are the same as those for  $r = 1 \forall r$ .

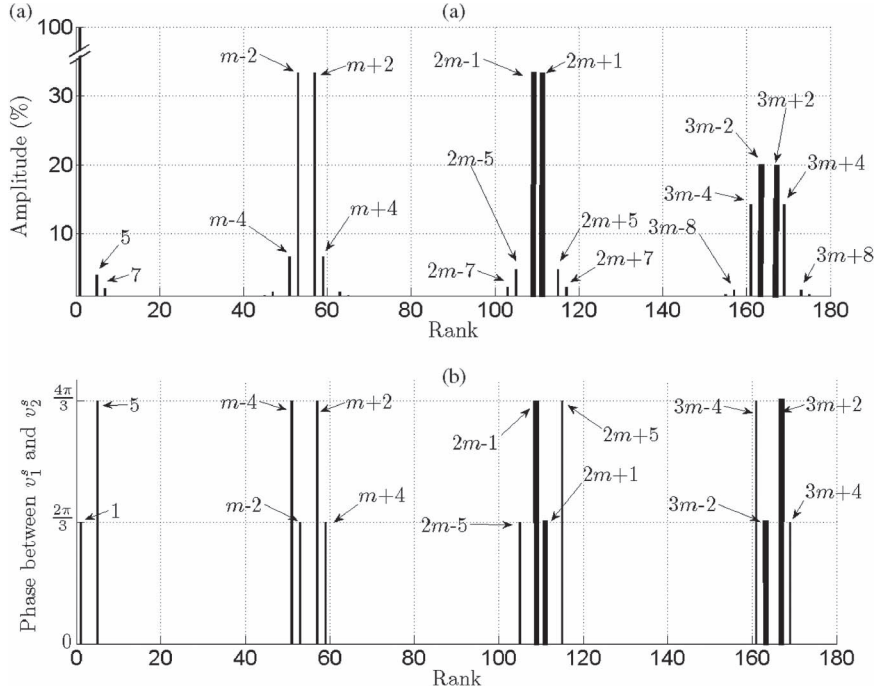


Fig. 4. Experimental  $v_q^s$  harmonic content for a single sinusoidal carrier ( $r = 1$ ).

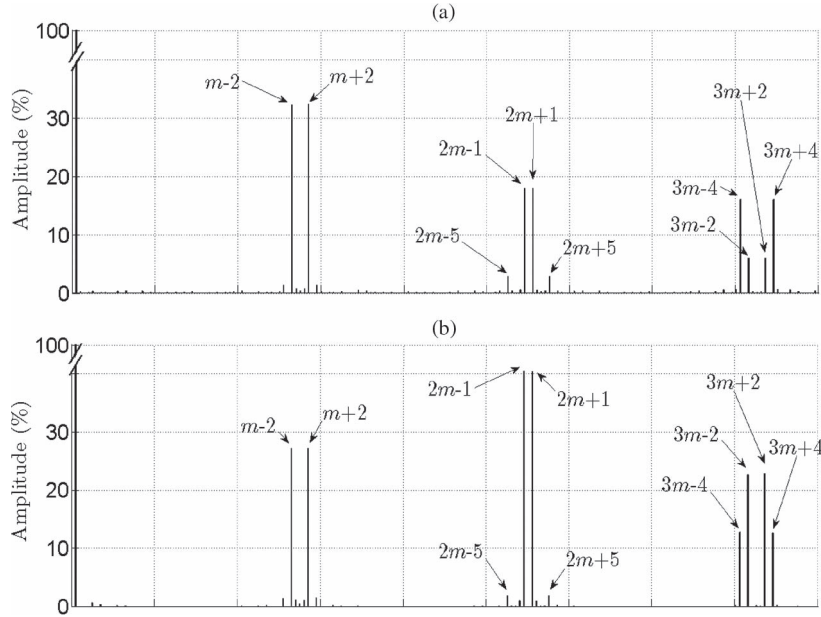


Fig. 5. Experimental  $v_q^\Delta$  harmonic content for a single triangular carrier ( $r = 1, 0.8$ ). (a)  $r = 1$ . (b)  $r = 0.8$ .

### B. Triangular Carrier

Fig. 5 shows the relative  $v_q^\Delta$  spectrum ( $\delta|\hat{v}_{q(k)}^\Delta|$ ,  $\hat{v}_{q(1)}^\Delta = rU_0/2 = 260$  V for  $r = 1$ ) for  $r = 1$  [see Fig. 5(a)] and  $r = 0.8$  [see Fig. 5(b)], which is experimentally obtained with a single triangular carrier. Comparing the  $\hat{v}_{q(k)}^\Delta$  relative amplitudes given in Figs. 4(a) and 5(a), it appears that, independent of the magnitude differences on the fundamental components according to the carrier type, sinusoidal and triangular carriers practically lead to the same harmonic ranks. The magnitude differences are notably amplified with the sinus–sinus PWM for components of low ranks (5 and 7), although they do not predominantly intervene on the spectral content. It is also noticeable that there is an inversion concerning the components of the highest am-

plitude around  $3m$ . The analysis of the phase sequences shows that they are independent from the carrier type and from the  $r$  and  $\xi_q$  values. Consequently, they can be always deduced from Fig. 4(b). This property can be expressed as follows: The phase angles at  $t = 0$  determined for a given  $\xi_q$ , which are calculated with the expression established for the sinus–sinus PWM and, thus, for  $r = 1$ , are also valuable for the harmonic components, which appear for the sinus–triangle PWM and this, whatever the value of  $r$  is. The fact that  $r$  does not intervene appears in [21]. That property is exploited in the following section. Compared with other methods [22], the method proposed by the authors allows simplifying the analytical expression of the PWM due to the use of logical functions. For example, it has the advantage

of not using a Fourier series with Bessel functions as for the double-Fourier series methods used in [23].

#### IV. VOLTAGE HARMONIC CONTROL

##### A. Principle of the Method

- Let us consider a harmonic of rank  $x$  belonging to the  $k_1$  group, which is denoted by  $k_1^{(x)}$ . This harmonic is defined by the  $[n_1^{(x)}, n_2^{(x)}]$  couple, which leads to the  $N^{+(x)}$  and  $N^{-(x)}$  quantities. Its expression, which is deduced from (7), is given by

$$w_q^s(k_1^{(x)}) = \hat{w}_{(k_1^{(x)})}^s \sin\left(k_1^{(x)}\theta - N^{-(x)}\phi_q - mN^{+(x)}\xi_q^{(x)}\right). \quad (14)$$

It becomes homopolar if  $N^{-(x)}\phi_q + mN^{+(x)}\xi_q^{(x)} = C_1^{(x)}\forall q$ , where  $C_1^{(x)}$  is a constant. It leads to

$$m\xi_q^{(x)} = \left(C_1^{(x)} - N^{-(x)}\phi_q\right) / N^{+(x)}. \quad (15)$$

When  $m\xi_q^{(x)}$  verifies (15), the modified STPH systems, which are also denoted by an upper index  $(x)$ , are given by (16), shown at the bottom of the page.

- The method is identical to cancel a  $k_2^{(x)}$ -rank harmonic belonging to the  $k_2$  group. Introducing a constant denoted by  $C_2^{(x)}$ , it can be deduced from (7) that, to make this STPH system (H), it suffices to satisfy the following equality:

$$m\xi_q^{(x)} = \left(C_2^{(x)} - N^{+(x)}\phi_q\right) / N^{-(x)} \quad (17)$$

so that the modified STPH systems are expressed as (18), shown at the bottom of the page.

- One can note that  $\xi_q^{(x)}$  depends on  $q$ . In addition,  $\xi_q^{(x)}$  does not modify the fundamental insofar as  $N^-$ , which multiplies  $\xi_q^{(x)}$ , is null. It appears that the coefficients of  $\phi_q$  are not necessarily integers, which means that the modified STPH systems become unbalanced. This imbalance only concerns the phase difference between the three terms, which present the same amplitudes. If the coefficients of  $\phi_q$  are integers, the modified STPH systems are still balanced, but their phase sequence can be changed.

Thereafter, the  $\xi_q^{(x)}$  values analytically determined with the sinus-sinus PWM will be used in the sinus-triangle PWM control to suppress a  $v_q^\Delta$  STPH system. As  $C_1^{(x)}$  and  $C_2^{(x)}$  have no influence *a priori*, they will be assumed to be null.

TABLE II  
THEORETICAL IMPACT OF THE SUPPRESSION OF THE  $m + 2$  RANK HARMONIC (GROUP  $k_2$ ) ON THE  $w_q^s$  SPECTRAL CONTENT

(a) $k_1 = n_1(m+1) + n_2(m-1) + m$					
$n_1$		0	1	2	3
$n_2$	0	m (H)→(C)	2m+1 (C)→(H)	3m+2 (A)	4m+3 (H)→(C)
	1	2m-1 (A)→(C)	3m (H)	4m+1 (C)→(A)	5m+2 (A)→(C)
	2	3m-2 (C)	4m-1 (A)→(H)	5m (H)→(A)	6m+1 (C)
	3	4m-3 (H)→(C)	5m-2 (C)→(H)	6m-1 (A)	7m (H)→(C)
(b) $k_2 = n_1(m+1) - n_2(m-1) + 1$					
$n_1$		0	1	2	3
$n_2$	0	1 (C)	m+2 (A)→(H)	2m+3 (H)→(A)	3m+4 (C)
	1	-m+2 (C)→(A)	3 (H)	m+4 (C)→(A)	2m+5 (A)→(C)
	2	-2m+3 (H)→(A)	-m+4 (A)→(H)	5 (A)	m+6 (H)→(C)
	3	-3m+4 (A)	-2m+5 (C)→(H)	-m+6 (H)→(C)	7 (C)

TABLE III  
THEORETICAL IMPACT OF THE  $m - 2$  HARMONIC ( $k_2$  GROUP) SUPPRESSION ON THE  $w_q^s$  SPECTRAL CONTENT

(a) $k_1 = n_1(m+1) + n_2(m-1) + m$					
$n_1$		0	1	2	3
$n_2$	0	m (H)→(A)	2m+1 (C)→(A)	3m+2 (A)	4m+3 (H)→(A)
	1	2m-1 (A)→(H)	3m (H)	4m+1 (C)→(H)	5m+2 (A)→(H)
	2	3m-2 (C)	4m-1 (A)→(C)	5m (H)→(C)	6m+1 (C)
	3	4m-3 (H)→(A)	5m-2 (C)→(A)	6m-1 (A)	7m (H)→(A)
(b) $k_2 = n_1(m+1) - n_2(m-1) + 1$					
$n_1$		0	1	2	3
$n_2$	0	1 (C)	m+2 (A)→(C)	2m+3 (H)→(C)	3m+4 (C)
	1	-m+2 (C)→(H)	3 (H)	m+4 (C)→(H)	2m+5 (A)→(H)
	2	-2m+3 (H)→(C)	-m+4 (A)→(C)	5 (A)	m+6 (H)→(A)
	3	-3m+4 (A)	-2m+5 (C)→(A)	-m+6 (H)→(A)	7 (C)

$$\begin{aligned} w_{q(k_1)}^s &= \hat{w}_{(k_1)}^s \sin \left\{ k_1\theta - \frac{1}{N^{+(x)}} \left[ (N^- N^{+(x)} - N^+ N^{-(x)}) \phi_q - \frac{N^+}{N^{+(x)}} C_1^{(x)} \right] \right\} \\ w_{q(k_2)}^s &= \hat{w}_{(k_2)}^s \sin \left\{ k_2\theta - \frac{1}{N^{+(x)}} \left[ (N^+ N^{+(x)} - N^- N^{-(x)}) \phi_q - \frac{N^-}{N^{+(x)}} C_1^{(x)} \right] \right\} \end{aligned} \quad (16)$$

$$\begin{aligned} w_{q(k_1)}^s &= \hat{w}_{(k_1)}^s \sin \left\{ k_1\theta - \frac{1}{N^{-(x)}} \left[ (N^- N^{-(x)} - N^+ N^{+(x)}) \phi_q - \frac{N^+}{N^{-(x)}} C_2^{(x)} \right] \right\} \\ w_{q(k_2)}^s &= \hat{w}_{(k_2)}^s \sin \left\{ k_2\theta - \frac{1}{N^{-(x)}} \left[ (N^+ N^{-(x)} - N^- N^{+(x)}) \phi_q - \frac{N^-}{N^{-(x)}} C_2^{(x)} \right] \right\} \end{aligned} \quad (18)$$

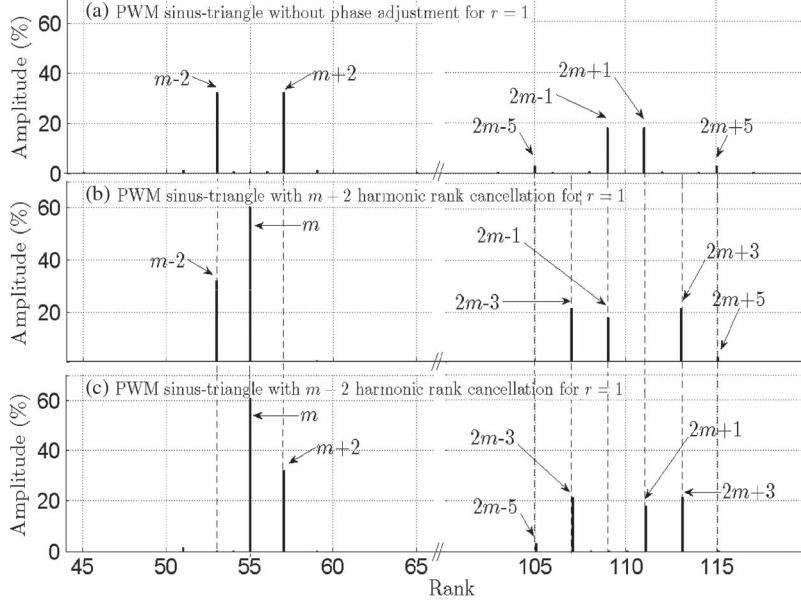


Fig. 6. Relative experimental  $v_q^\Delta$  spectra resulting from (b)  $m+2$  and (c)  $m-2$  rank harmonic cancellations for  $r=1$ .

### B. Cancellation of Harmonic Around $m$ ( $k_2$ Group)

- Let us assume that one choice to suppress the  $m+2$  rank is the (A) STPH system that belongs to the  $k_2$  group. It is denoted by  $k_2^{(m+2)}$ , and it is defined for  $n_1^{(m+2)} = 1$  and  $n_2^{(m+2)} = 0$  (see Table I). That leads to  $N^{+(m+2)} = 2$  and  $N^{-(m+2)} = 1$ . This STPH system, which was deduced from (7), is expressed as

$$w_q^s(k_2^{(m+2)}) = \hat{w}_{k_2^{(m+2)}}^s \sin(k_2^{(m+2)}\theta + \phi_q - m\xi_q^{(m+2)}). \quad (19)$$

To obtain an (H) system, expression (19) leads to

$$\xi_q^{(m+2)} = \phi_q/m. \quad (20)$$

The modified STPH systems can be expressed as

$$\left. \begin{aligned} w_q^s(k_1) &= \hat{w}_{k_1}^s \sin[k_1\theta - (1+2n_1)\phi_q] \\ w_q^s(k_2) &= \hat{w}_{k_2}^s \sin[k_2\theta - (1+2n_1)\phi_q] \end{aligned} \right\}. \quad (21)$$

It can be noted that the phase sequences only depend on  $n_1$  and, for the terms of the  $k_2$  group, on the sign of  $k_2$ . Table II presents the  $w_q^s$  analytical spectral content modifications, which only concern the system phase sequences. For instance, (H)  $\rightarrow$  (C) means that a system that is initially (H) becomes (C). It appears that the harmonic components, which do not depend on  $m$ , and those around  $3m$  and  $6m$  keep the same characteristics (see the grayed cells in Table III). When the  $m+2$  component disappears, other terms are suppressed, but, in return, other components appear as the component of rank  $m$ , which presents a high amplitude because it is defined for  $n_1 = n_2 = 0$ .

From an experimental point of view, the Focusrite sound card has been programmed to generate three triangular carriers with  $m=55$  and  $\xi_q^{(m+2)}$  given by (20). Fig. 6 shows the relative  $v_1^\Delta$  experimental spectrum without [see Fig. 6(a)] and with [see Fig. 6(b)] the harmonic cancellation. It shows that the properties concerning the suppression or the generation of STPH systems are verified. It confirms that the law established

for the sinus-sinus PWM is also true for the sinus-triangle PWM. On the other hand, there is still the problem concerning the amplitudes. Fig. 7 shows that the same properties are found for  $r=0.8$  than for  $r=1$ .

It means that the phase sequence is independent of  $r$ . The modeling method to find the phase shift of the three carriers for canceling an STPH system stays valid whatever  $r$  is.

- The same procedure can be used to suppress the  $m-2$  rank (C) STPH system. It shows that, to get an (H) system,  $\xi_q^{(m-2)}$  must be equal to

$$\xi_q^{(m-2)} = -\phi_q/m \quad (22)$$

so that the modified STPH systems can be written as:

$$\left. \begin{aligned} w_q^s(k_1) &= \hat{w}_{k_1}^s \sin[k_1\theta + (1+2n_2)\phi_q] \\ w_q^s(k_2) &= \hat{w}_{k_2}^s \sin[k_2\theta - (1+2n_2)\phi_q] \end{aligned} \right\}. \quad (23)$$

- In this case, the phase sequence only depends on  $n_2$  and on the sign of  $k_2$ . Table III presents the  $w_q^s$  analytical spectral content modifications, which only concern the system phase sequences. The same terms as earlier keep the same characteristics (see the grayed cells in Table III).

Fig. 6 shows the relative amplitudes of the  $v_1^\Delta$  experimental spectra without [see Fig. 6(a)] and with [see Fig. 6(c)] the harmonic suppression for  $\xi_q^{(m-2)}$  given by (22) and  $r=1$ .

### C. Cancellation of Harmonic Around $2m$ ( $k_1$ Group)

In this case, only the case where  $r=1$  will be studied.

- The harmonic of rank  $2m+1$  is considered. Its rank, which is denoted by  $k_1^{(2m+1)}$ , is defined for  $n_1^{(2m+1)} = 1$  and  $n_2^{(2m+1)} = 0$  that gives  $N^{+(2m+1)} = 2$  and  $N^{-(2m+1)} = 1$ , respectively. This (C) STPH system, which was deduced from (7), is given by

$$w_q^s(k_1^{(2m+1)}) = \hat{w}_{k_1^{(2m+1)}}^s \sin(k_1^{(2m+1)}\theta - \phi_q - 2m\xi_q^{(2m+1)}). \quad (24)$$

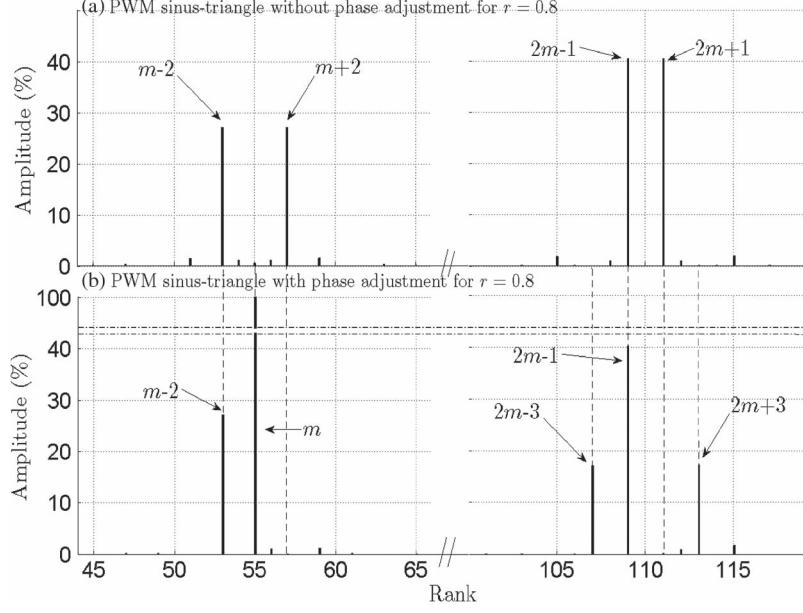


Fig. 7. Relative experimental  $v_q^\Delta$  spectra resulting from  $m + 2$  rank harmonic cancellation for  $r = 0.8$ .

TABLE IV  
THEORETICAL IMPACT OF THE  $2m + 1$  HARMONIC (GROUP  $k_1$ )  
SUPPRESSION ON THE  $w_q^s$  SPECTRAL CONTENT

(a) $k_1 = n_1(m+1) + n_2(m-1) + m$					
$n_1$	0	1	2	3	
$n_2$	0	m (H)→(HCA)	2m+1 (C)→(H)	3m+2 (A)→(HCA)	4m+3 (H)→(C)
	1	2m-1 (A)→(C)	3m (H)→(HCA)	4m+1 (C)→(A)	5m+2 (A)→(HCA)
	2	3m-2 (C)→(HCA)	4m-1 (A)→(H)	5m (H)→(HCA)	6m+1 (C)
	3	4m-3 (H)→(C)	5m-2 (C)→(HCA)	6m-1 (A)	7m (H)→(HCA)
(b) $k_2 = n_1(m+1) - n_2(m-1) + 1$					
$n_1$	0	1	2	3	
$n_2$	0	1 (C)	m+2 (A)→(HCA)	2m+3 (H)→(A)	3m+4 (C)→(HCA)
	1	-m+2 (C)→(HCA)	3 (H)	m+4 (C)→(HCA)	2m+5 (A)→(C)
	2	-2m+3 (H)→(A)	-m+4 (A)→(HCA)	5 (A)	m+6 (H)→(HCA)
	3	-3m+4 (A)→(HCA)	-2m+5 (C)→(H)	-m+6 (H)→(HCA)	7 (C)

To make it homopolar,  $\xi_q^{(2m+1)}$  must be equal to

$$\xi_q^{(2m+1)} = -\phi_q/2m. \quad (25)$$

The modified STPH systems can be expressed as follows:

$$\left. \begin{aligned} w_{q(k_1)}^{s(2m+1)} &= \hat{w}_{(k_1)}^s \sin\left(k_1\theta - \frac{n_1 - 3n_2 - 1}{2}\phi_q\right) \\ w_{q(k_2)}^{s(2m+1)} &= \hat{w}_{(k_2)}^s \sin\left(k_2\theta - \frac{n_1 + 3n_2 + 2}{2}\phi_q\right) \end{aligned} \right\}. \quad (26)$$

In that case, many systems that are initially balanced become unbalanced. Table IV shows the modifications of the STPH system phase sequences. (HCA) means that a system that is initially (C), (A), or (H) becomes unbalanced. Only the harmonic components, which do not depend on  $m$ , and those around  $6m$  keep the same characteristics (see the grayed cells in Table IV). In that case, the comparison with the experimental measurements is more complicated

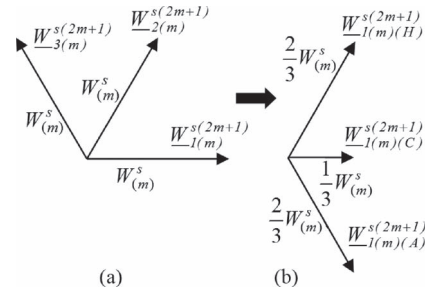


Fig. 8. Suppression of the  $2m + 1$  harmonic: Characterization of the (C), (A), and (H) components of the rank  $m$  unbalanced system.

insofar as most of the STPH systems are unbalanced. It is thus necessary to characterize each of them with its (C), (A), and (H) components, which result from the following classical expressions if phase 1 is considered, which use time phasor variables and where  $a = \exp(j2\pi/3)$ :

$$\left. \begin{aligned} \underline{W}_{1(k)(C)}^{s(x)} &= \left( \underline{W}_{1(k)}^{s(x)} + a\underline{W}_{2(k)}^{s(x)} + a^2\underline{W}_{1(k)}^{s(x)} \right) / 3 \\ \underline{W}_{1(k)(A)}^{s(x)} &= \left( \underline{W}_{1(k)}^{s(x)} + a^2\underline{W}_{2(k)}^{s(x)} + a\underline{W}_{1(k)}^{s(x)} \right) / 3 \\ \underline{W}_{1(k)(H)}^{s(x)} &= \left( \underline{W}_{1(k)}^{s(x)} + \underline{W}_{2(k)}^{s(x)} + \underline{W}_{1(k)}^{s(x)} \right) / 3 \end{aligned} \right\}. \quad (27)$$

Let us consider, for example, the  $k_1$  group unbalanced system defined for  $n_1 = n_2 = 0$ , i.e.,  $k_1 = m$ . Using the first expression of (26), it can be written as

$$w_{q(m)}^{s(2m+1)} = \hat{w}_{(m)}^s \sin(m\theta + (q-1)\pi/3). \quad (28)$$

It leads to Fig. 8(a), where the modulus of each time phasor variable is  $W_{(m)}^s = \hat{w}_{(m)}^s/\sqrt{2}$ . Using (27) leads to the phase 1 time phasor variable of each component given in Fig. 8(b). It can be noted that the (H) and (A) systems have the same modulus equal to  $2W_{(m)}^s/3$ , whereas the (C) modulus is  $W_{(m)}^s/3$ . As, theoretically, the relative value of the  $m$  harmonic is equal to 1 (see Table I), it can be deduced that the relative absolute values of the (C) and (A) systems of  $v_{(m)}^{s(2m+1)}$  are 33.3%

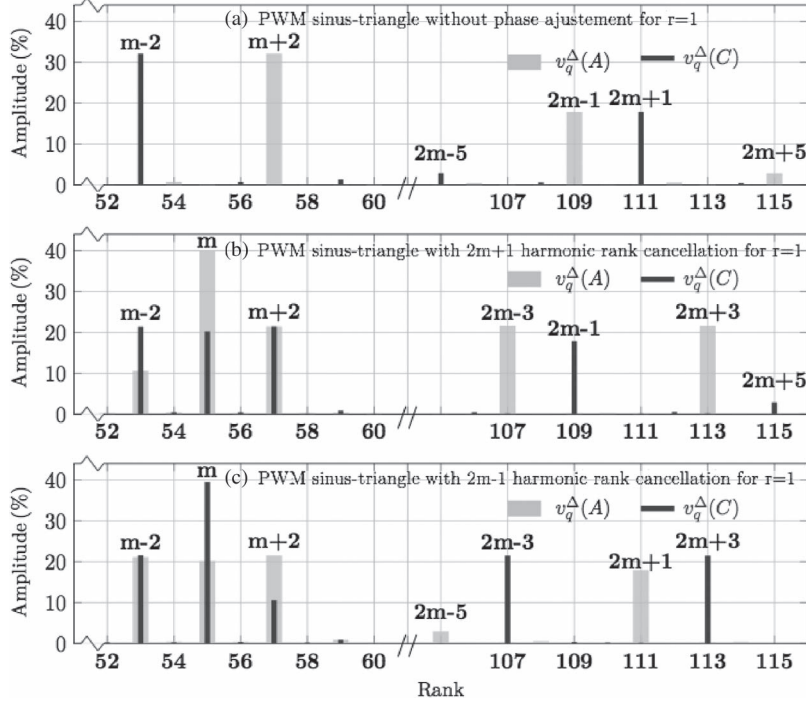


Fig. 9. Relative experimental  $v_{q(C)}^{\Delta}$  and  $v_{q(A)}^{\Delta}$  spectra resulting from the (b)  $2m + 1$  and (c)  $2m - 1$  rank harmonic cancellations for  $r = 1$ .

and 66.6%, respectively. Fig. 9 shows the relative amplitudes of the  $v_1^{\Delta}$  experimental spectra without [see Fig. 9(a)] and with [see Fig. 9(b)] the harmonic suppression considering the  $v_{q(C)}^{\Delta}$  and  $v_{q(A)}^{\Delta}$  components, which were determined from the measurements and the analysis of the  $v_q^{\Delta}$  system for  $\xi_q^{(2m+1)}$  given by (25).

- In order to cancel the  $2m - 1$  rank, i.e., (A) STPH system, one has to satisfy the following equality:

$$\xi_q^{(2m-1)} = \phi_q/2m. \quad (29)$$

This leads to the modified STPH systems as follows:

$$\left. \begin{aligned} w_{q(k_1)}^{s(2m-1)} &= \hat{w}_{(k_1)}^s \sin(k_1\theta - \frac{3n_1-n_2+1}{2}\phi_q) \\ w_{q(k_2)}^{s(2m-1)} &= \hat{w}_{(k_2)}^s \sin(k_2\theta - \frac{3n_1+n_2+2}{2}\phi_q) \end{aligned} \right\}. \quad (30)$$

It can be shown that, as for the previous case, the components, which are not influenced, are those that do not depend on  $m$  and those of rank around  $6m$ . By considering the  $k_1$  group STPH system of rank  $m$ , it can be written as

$$w_{q(m)}^{s(2m-1)} = \hat{w}_{(m)}^s \sin(m\theta - (q-1)\pi/3). \quad (31)$$

In a similar way, the use of the time phasor leads to the (C) and (A) component relative values that are equal to 66.6% and 33.3%, respectively. The relative importance of these systems is changed compared with the previous case.

Fig. 9(c) shows the relative amplitudes of the  $v_{q(C)}^{\Delta}$  and  $v_{q(A)}^{\Delta}$  spectra, which were determined from the measurements and the analysis of the  $v_q^{\Delta}$  system obtained for  $\xi_q^{(2m-1)}$  given by (29).

- The suppression of the component of rank  $2m + 1$  or  $2m - 1$  leads to new components of rank  $2m \pm 3$ , which are both (C) and (A), as determined with the analytical

model. Contrary to the suppressions of the  $m + 2$  and  $m - 2$  components, the rank  $m$  component is separated into (C) and (A) components. The amplitudes of the latter are reduced, but their sum, without any physical significance, is always equal to 100%.

## V. APPLICATION TO CONTROL OF RADIAL VIBRATIONS

The following study is simplified insofar as the toothing effect is not taken into account. Each  $v_{q(k)}^{\Delta}$  STPH system generates a  $b_{(k)}^{\Delta}$  harmonic rotating magnetic field. Because of the definition of Maxwell's forces, only the components that result from the  $b_{(1)}^{\Delta} b_{(k)}^{\Delta}$  products are considered. In these conditions, the force frequencies are given by  $(k \pm 1)f$ . The spectral analysis of the radial accelerations show that the switching effect appear at frequencies located around  $2m, 3m, \dots$ . The experimental accelerations of the vibrations situated around  $2m$  and the acoustic pressure measured at 80 cm from the machine in a semianechoic room are presented in Fig. 10(a). Table I shows that the ranks of the STPH systems that must be considered are  $2m \pm 1$  (the  $k_1$  group) and  $2m \pm 3$  (the  $k_2$  group). This leads to the following force frequencies:

$$2m-1 \rightarrow 5400 \text{ Hz}, 5500 \text{ Hz}; \quad 2m+1 \rightarrow 5500 \text{ Hz}, 5600 \text{ Hz};$$

$$2m-3 \rightarrow 5300 \text{ Hz}, 5400 \text{ Hz}; \quad 2m+3 \rightarrow 5600 \text{ Hz}, 5700 \text{ Hz}.$$

It can be emphasized that a force component is not associated to a unique STPH system. Therefore, with this simplified analysis, it is not possible to determine which force component has the highest amplitude, although the experimental measurements show that 5500 and 5600 Hz have overriding effects. The 5300- and 5700-Hz components have low amplitudes, which can be explained by the (H) nature of the  $2m \pm 3$  STPH systems.

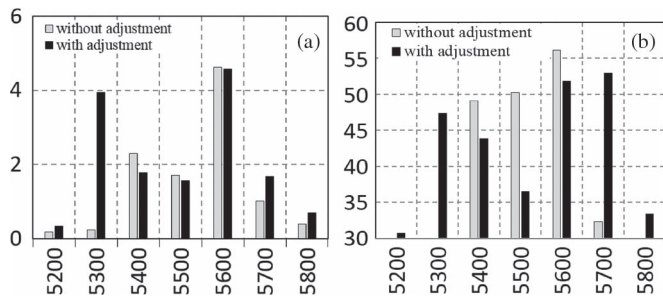


Fig. 10. (a) Acceleration (in meters per second squared) of the vibrations. (b) Acoustic noise (in A-weighted decibels) without and with carrier phase adjustment with frequency (in Hertz).

Let us suppose that the 5600-Hz force component has to be reduced. It can be done by changing the  $2m + 1$  STPH system in (H). The study presented in Section IV-C explains the control, and Table IV shows that the  $2m \pm 3$  STPH systems, which were initially (H), become (A) and that the (A)  $(2m - 1)$  STPH systems become (C). In fact, concerning these components, the same result can be obtained by making (H) the  $(m + 2)$  STPH system (see Table II). As a result, the phase adjustment can be chosen. Applying the value given by (20) leads to the experimental spectra shown in Fig. 10(b). In terms of noise, the 5600-, 5500-, and 5400-Hz components are reduced of 4, 13, and 5 dBA, respectively, whereas the 5300- and 5700-Hz components are increased because the  $2m \pm 3$  STPH systems, which were initially (H), become (A). Consequently, these components, which are negligible without the phase adjustment, have amplitudes of 47.5 and 53 dBA, respectively. These variations are in accordance with the theory. Practically, the aim of the method is to control noise components with frequencies close to a natural resonance. In that case, their amplitudes are greatly amplified, which is not the case for the considered example.

## VI. CONCLUSION

In this paper, the authors have proposed to reduce some undesirable effects generated by the switching. The principle is to suppress some annoying STPH systems of the output sinus-triangle PWM. To do that, the phase sequences of all the STPH systems have to be determined to define a control, making some of them homopolar. Thus, the authors have developed an analytical model based on an associated “sinus-sinus” PWM. It is shown that this model makes accurate phase sequence determination possible and that the results remain valid for the sinus-triangle PWM whatever the modulation index and the adjusting index are. Based on this property, the authors present the control strategy that uses three distinct carriers. The experiments confirm the theoretical developments and point out the possibility to analyze the impact of the STPH cancelation on other uncanceled harmonic components, which is an aspect that is not often studied in literature. That method, which is based on analytical formulation, is used to modify the induction machine’s radial vibrations. It constitutes the basis for further studies as the possibility to simultaneously act on several harmonic components.

## REFERENCES

- [1] P. Marian, L. G. Franquelo, J. Rodriguez, M. A. Perez, and J. I. Leon, “High-performance motor drives,” *IEEE Ind. Electron. Mag.*, vol. 5, no. 3, pp. 6–26, Sep. 2011.
- [2] D. G. Holmes and T. A. Lipo, *Pulse Width Modulation for Power Converters—Principles and Practice*. Hoboken, NJ, USA: Wiley, 2003.
- [3] E. R. C. da Silva, E. C. dos Santos, and C. B. Jacobina, “Pulsewidth modulation strategies,” *IEEE Ind. Electron. Mag.*, pp. 37–45, Jun. 2011.
- [4] S. Khomfoi, V. Kinnaree, and P. Viriya, “Influence of PWM characteristics on the core losses due to harmonic voltages in PWM fed induction motors,” in *Proc. Power Eng. Soc. Winter Meet.*, 2000, vol. 1, pp. 365–369.
- [5] S. Iida, Y. Okuma, S. Masukawa, S. Miyairi, and B. K. Bose, “Study on magnetic noise caused by harmonics in output voltages of PWM inverter,” *IEEE Trans. Ind. Electron.*, vol. 38, no. 3, pp. 180–186, Jun. 1991.
- [6] P. Pellerey, G. Favennec, V. Lanfranchi, and G. Friedrich, “Active reduction of electrical machines magnetic noise by the control of low frequency current harmonics,” in *Proc. 38th IEEE IECON*, Oct. 2012, pp. 1654–1659.
- [7] V. Mihaila, S. Duchesne, and D. Roger, “A simulation method to predict the turn-to-turn voltage spikes in a PWM fed motor winding,” *IEEE Trans. Dielectr. Electr. Insul.*, vol. 18, no. 5, pp. 1609–1615, Oct. 2011.
- [8] M. Malinowski, K. Gopakumar, J. Rodriguez, and M. A. Pérez, “A survey on cascaded multilevel inverters,” *IEEE Trans. Ind. Electron.*, vol. 57, no. 7, pp. 2197–2206, Jul. 2010.
- [9] J. Le Besnerais, V. Lanfranchi, and P. Brochet, “Characterization and reduction of audible magnetic noise due to PWM supply in induction machines,” *IEEE Trans. Ind. Electron.*, vol. 57, no. 4, pp. 1288–1295, Apr. 2010.
- [10] D.-J. Kim, J.-W. Jung, J.-P. Hong, K.-J. Kim, and C.-J. Park, “A Study on the design process of noise reduction in induction motors,” *IEEE Trans. Magn.*, vol. 48, no. 11, pp. 4638–4641, Nov. 2012.
- [11] N. Hashemi, R. Lisner, and D. Holmes, “Acoustic noise reduction for an inverter-fed three-phase induction motor,” in *Proc. 39th IEEE IAS Annu. Meeting*, Oct. 2004, pp. 2030–2035.
- [12] T. G. Habetler and D. M. Divan, “Acoustic noise reduction in sinusoidal PWM drives using a randomly modulated carrier,” *IEEE Trans. Power Electron.*, vol. 6, no. 3, pp. 356–363, Jul. 1991.
- [13] G. A. Covic and J. T. Boys, “Noise quieting with random PWM AC drives,” *Proc. Inst. Elect. Eng.—Elect. Power Appl.*, vol. 145, pp. 1–10, 1998.
- [14] J. C. Lai and C. Wang, “Prediction of noise radiation from induction motors,” in *Proc. 6th Int. Congr. Sound Vibration*, Copenhagen, Denmark, Jul. 1999, pp. 2449–2456.
- [15] E. Leleu, C. Espanet, A. Miraoui, and S. Siala, “Reduction of vibrations in an induction machine supplied by high power PWM inverter,” in *Proc. Eur. Conf. Power Electron. Appl.*, 2005, pp. 1–8.
- [16] A. Ruiz-Gonzalez, M. J. Meco-Gutierrez, F. Perez-Hidalgo, F. Vargas-Merino, and J. R. Heredia Larrubia, “Reducing acoustic noise radiated by inverter-fed induction motors controlled by a new PWM strategy,” *IEEE Trans. Ind. Electron.*, vol. 57, no. 1, pp. 228–236, Jan. 2010.
- [17] J.-F. Brudny and J.-Ph. Lecoine, “Rotor design for reducing the switching magnetic noise of AC electrical machine variable-speed drives,” *IEEE Trans. Ind. Electron.*, vol. 58, no. 11, pp. 5112–5120, Nov. 2011.
- [18] H. Tischmacher and B. Eichinger, “Sound optimisation of a converter-fed drive system using an acoustic camera in combination with modal analysis,” in *Proc. COMPEL*, 2010, vol. 29, no. 4, p. 908.
- [19] J. Ojeda, X. Mininger, and M. Gabsi, “An active piezoelectric absorber for vibration control of electrical machine,” in *Proc. IEEE ICIT*, Feb. 2013, pp. 234–241.
- [20] C. Demian, B. Cassoret, J. F. Brudny, and T. Belgrand, “AC magnetic circuits using non segmented shifted grain oriented electrical steel sheets: Impact on induction machine magnetic noise,” *IEEE Trans. Magn.*, vol. 48, no. 4, pp. 1409–1412, Apr. 2012.
- [21] S. R. Bowes, “New sinusoidal pulsewidth-modulated inverter,” *Proc. Inst. Elect. Eng.*, vol. 122, no. 11, pp. 1279–1285, Nov. 1975.
- [22] D. G. Holmes, “A general analytical method for determining the theoretical harmonic components of carrier based PWM strategies,” in *Proc. 33rd IEEE IAS Annu. Meeting*, 1998, vol. 2, pp. 1207–1214.
- [23] J. Sun and H. Grotstollen, “Fast time-domain simulation by waveform relaxation methods,” *IEEE Trans. Circuits Syst. I, Fundam. Theory Appl.*, vol. 44, no. 8, pp. 660–666, Aug. 1997.



**Jean-François Brudny** (M'92–SM'04) received the Ph.D. and D.Sc. degrees from Lille University, Villeneuve d'Ascq, France, in 1984 and 1991, respectively.

In 1992, he joined Artois University (UArtois), Béthune, France, as a Full Professor, and he is currently the Head of the Laboratoire Systèmes Electrotechniques et Environnement (LSEE). His research interests include noise and vibrations of electromechanical systems and new designs for the efficiency increase of ac rotating

electrical machines.



**Fabrice Morganti** was born in 1965. He received the Ph.D. degree from Lille-I University, France, in 1994.

He is currently an Associate Professor with Artois University (UArtois), Béthune, France, where he joined Laboratoire Systèmes Electrotechniques et Environnement (LSEE). His research interests include signal processing and electromagnetic design.



**Tifany Szkudlapski** is currently working toward the Ph.D. degree at the Laboratoire Systèmes Electrotechniques et Environnement, Artois University, Béthune, France.

His research interests include noise and vibrations of electrical machines.



**Jean-Philippe Lecointe** (M'04) received the M.Sc. degree in electrical engineering from Lille University, France, in 2000 and the Ph.D. and D.Sc. degrees from Artois University, France, in 2003 and 2012, respectively.

He is currently a Full Professor with the Laboratoire Systèmes Electrotechniques et Environnement (LSEE), Artois University. His research interests include electromagnetic design, and the efficiency and noise of electrical machines.